Mechanistic Studies on the Formation of η^2-Diphosphine (η^6-*p*-cymene)ruthenium(II) Compounds

Adrian B. Chaplin, Céline Fellay, Gábor Laurenczy, and Paul J. Dyson*

Institut des Sciences et Ingénierie Chimiques, Ecole Polytechnique Fédérale de Lausanne (EPFL), CH-1015 Lausanne, Switzerland

Received August 21, 2006

A new range of pendent diphosphine (η^6-*p*-cymene)ruthenium(II) complexes, [RuCl(PPh_3)(η^1-(P−P))-(η^6-*p*-cymene)]PF_6 (P−P = dppm, *cis*-$PPh_2CHCHPPh_2$ (dppv), dppe, dppp, dppf), have been prepared by substitution of the labile acetonitrile ligand in [RuCl(CH_3CN)(PPh_3)(η^6-*p*-cymene)]PF_6. The formation of chelate complexes, [RuCl(η^2-(P−P))(η^6-*p*-cymene)]$^+$, from these pendent phosphine complexes and from the related neutral complexes, [$RuCl_2$(η^1-(P−P))(η^6-*p*-cymene)] (P−P = dppm, dppv), has been investigated, including determination of activation enthalpies ($\Delta H^{\ddagger}$) and entropies ($\Delta S^{\ddagger}$). A concerted substitution mechanism is proposed for the latter complexes, in which methanol plays an important role in the ring-closing process by formation of hydrogen bonds with the chloride ligands. This proposal is supported by volumes of activation ($\Delta V^{\ddagger}$) determined by variable-pressure UV−visible spectroscopy. In contrast, a dissociative mechanism is proposed for the series of cationic pendent phosphine complexes, which generally require higher temperatures to effect ring closure. Secondary reaction pathways can be observed in some cases and are discussed in terms of differences between the phosphine complexes and supplemented by investigations using electrospray ionization mass spectrometry (ESI-MS). The X-ray structures of [RuCl(PPh_3)(η^1-(P−P))(η^6-*p*-cymene)]PF_6 (P−P = dppm, dppv, dppp) and [RuCl(η^2-dppv)-(η^6-*p*-cymene)]PF_6 are also reported.

Introduction

Half-sandwich ruthenium(II)−η^6-arene complexes are an important and widely used class of organometallic compound, which exhibit a diverse range of coordination chemistry and show considerable potential as precursors for catalytic organic transformations.[1−4] In particular, complexes of this nature bearing chelating ligands, [RuX(η^6-arene)(L−L′)]$^+$, have well-demonstrated catalytic utility and are of current interest for a variety of asymmetric reactions.[2,3] Complexes bearing bidentate phosphine ligands represent an important subgroup[3] and, as well as finding various applications in catalysis, show considerable potential as catalysts in biphasic hydrogenation reactions.[4]

While the use of bidentate phosphine ligands is prevalent in the coordination chemistry of the transition metals, it is interesting to note that the actual process of forming these complexes has received relatively little attention. The chelation reactions for a variety of bidentate phosphine ligands on metal carbonyl complexes of group VI (eq 1)[5] and recently in those of ruthenium (eq 2)[6] have previously been investigated and found to proceed with varying degrees of bond breaking and making. For ruthenium, entropies of activation range from 63 to −13 J mol^{-1} K^{-1} and were taken to imply a mechanism with predominately dissociative to significantly associative character along the series PPh_2(*o*-C_6H_4)PPh_2 < $Cy_2P(CH_2)_2PCy_2$ < $Me_2P(CH_2)_2PMe_2$ < dppp ≤ dppm ≈ dppb ≈ dppe ≪ PPh_2(NMe)PPh_2.[7] The reaction between monodentate phosphine ligands and the widely used ruthenium(II) precursor [$RuCl_2$-(η^6-*p*-cymene)]$_2$, a well-established route to complexes of the type [$RuCl_2$(PR_3)(η^6-*p*-cymene)] (eq 3), has been investigated in detail by Serron and Nolan.[8] They measured the enthalpy of

* Corresponding author. E-mail: paul.dyson@epfl.ch.

(1) For examples see: (a) Rigby, J. H.; Kondratenko, M. A. *Top. Organomet. Chem.* **2004**, *7*, 181−204. (b) Bennett, M. A. *Coord. Chem. Rev.* **1997**, *166*, 225−254. (c) Bennett, M. A. *Comprehensive Organometallic Chemistry II*; Abel, E. W., Stone, F. G. A., Wilkinson, G., Eds.; Elsevier: Oxford, 1995, Vol. 7, pp 549−602. (d) Le Bozec, H.; Touchard, D.; Dixneuf, P. H. *Adv. Organomet. Chem.* **1989**, *29*, 163−247. (e) Naota, T.; Takaya, H.; Murahashi, S.-I. *Chem. Rev.* **1998**, *98*, 2599−2660. (f) Bustelo, E.; Dixneuf, P. H. *Adv. Synth. Catal.* **2005**, *347*, 393−397. (g) Castarlenas, R.; Dixneuf, P. H. *Angew. Chem., Int. Ed.* **2003**, *42*, 4524−4527, and references therein. (h) Farrington, E. J.; Brown, J. M.; Barnard, C. F. J.; Rowsell, E. *Angew. Chem., Int. Ed.* **2002**, *41*, 169−171. (i) Akiyama, R.; Kobayashi, S. *Angew. Chem., Int. Ed.* **2002**, *41*, 2602−2604. (j) Simal, F.; Demonceau, A.; Noels, A. F. *Angew. Chem., Int. Ed.* **1999**, *38*, 538−540.

(2) For illustrative examples see: (a) Noyori, R.; Hashiguchi, S. *Acc. Chem. Res.* **1997**, *30*, 97−102. (b) Hannedouche, J.; Clarkson, G. J.; Wills, M. *J. Am. Chem. Soc.* **2004**, *126*, 986−987. (c) Geldbach, T. J.; Dyson, P. J. *J. Am. Chem. Soc.* **2004**, *126*, 8114−8115. (d) Zhou, Y.-G.; Tang, W.; Wangm, W.-B.; Li, L.; Zhang, X. *J Am. Chem. Soc.* **2002**, *124*, 4952−4953.

(3) (a) Qiu, L.; Kwong, Y.; Wu, J.; Lam, W. H.; Chan, S. Yu, W.-Y.; Li, Y.-M.; Guo, R.; Zhou, Z.; Chan, A. S. C. *J. Am. Chem. Soc.* **2006**, *128*, 5955−5965. (b) Mashima, K.; Kusano, K.-H.; Sato, N.; Matsumura, Y.-I.; Nozaki, K.; Kumobayashi, H.; Sayo, N.; Hori, Y.; Ishizaki, T.; Akutagawa, S.; Takaya, H. *J. Org. Chem.* **1994**, *59*, 3064−3076. (c) Mashima, K.; Matsumura, Y.-I.; Kusano, K.-H.; Kumobayashi, H.; Sayo, N.; Hori, Y.; Ishizaki, T.; Akutagawa, S.; Takaya, H. *J. Chem. Soc., Chem. Commun.* **1991**, 609−610. (d) Mashima, K.; Kusano, K.-H.; Ohta, T.; Noyori, R.; Takaya, H. *J. Chem. Soc., Chem. Commun.* **1989**, 1208−1210.

(4) (a) Daguenet, C.; Scopelliti, R.; Dyson, P. J. *Organometallics* **2004**, *23*, 4849−4857. (b) Daguenet, C.; Dyson, P. J. *Organometallics* **2004**, *23*, 6080−6083. (c) Ghebreyessus, K. Y.; Nelson, J. H. *J. Organomet. Chem.* **2003**, *669*, 48−56. (d) Daguenet, C.; Dyson, P. J. *Catal. Commun.* **2003**, *4*, 153−157.

(5) (a) Connor, J. A.; Day, J. P.; Jones, E. M.; McEwen, G. K. *J. Chem. Soc., Dalton Trans.* **1973**, 347−354. (b) Connor, J. A.; Riley, P. I. *J. Organomet. Chem.* **1975**, *94*, 55−60.

(6) Bunten, K. A.; Farrar, D. H.; Poë, A. J.; Lough, A. J. *Organometallics* **2000**, *19*, 3674−3682.

(7) Abbreviations used for diphosphines and related ligands: $PPh_2CH_2PPh_2$ (dppm), *cis*-$PPh_2CHCHPPh_2$ (dppv), $PPh_2(CH_2)_2PPh_2$ (dppe), $PPh_2(CH_2)_3PPh_2$ (dppp), 1,1′-bis(diphenylphosphino)ferrocene (dppf), [(*S*)-2-(dimethylamino)-3-phenylpropyl]diphenylphosphine (*S*-phephos).

(8) Serron, S. A.; Nolan, S. P. *Organometallics* **1995**, *14*, 4611−4616.

10.1021/om060752n CCC: $37.00 © 2007 American Chemical Society
Publication on Web 12/15/2006

Table 1. Selected ^{1}H, ^{13}C, and ^{31}P NMR Data for Complexes 1 and [2a−e]PF_6 ($CDCl_3$, 293 K)[a]

	1	[2a]PF_6	[2b]PF_6	[2c]PF_6	[2d]PF_6	[2e]PF_6
ligand	CH_3CN	dppm	dppv	dppe	dppp	dppf
H^7	1.75	0.93	0.99	0.84	0.85	1.10
H^8	3.05	2.78	2.58	2.76	2.76	2.67
$\Delta[H^9, H^{10}]$	0.02	0.06	0.19	0.07	0.05	0.19
C^1	103.6	98.7	100.6	98.8	99	99
C^4	116.6	132	130	132	132	132
PPh_3	35.5	23.0	25.8	23.2[b]	23.2	23.3
Ru-PPh_2		22.0	7.4	23.0[b]	18.4	19.7
$^2J_{PP}$[c]		52	55	52[b]	52	52
pend-PPh_2		−28.8	−33.2	−13.0	−18.1	−19.4
J_{PP}[d]		44	15	26		

[a] Labels as in Scheme 1. [b]From simulation analysis. [c] ^2J(*P*Ph_3, η^1-(*P*−P)). [d] J(η^1-(*P*−P), η^1-(P−*P*)).

reaction for these reactions by solution calorimetry and found significant dependence on both steric and electronic factors.

$$[M(CO)_5(\eta^1\text{-}(P{-}P))] \rightarrow [M(CO)_4(\eta^2\text{-}(P{-}P))] + CO \quad (1)$$

$$[Ru(CO)_4(\eta^1\text{-}(P{-}P))] \rightarrow [Ru(CO)_3(\eta^2\text{-}(P{-}P))] + CO \quad (2)$$

$$[RuCl_2(\eta^6\text{-}p\text{-cymene})]_2 + 2PR_3 \rightarrow 2[RuCl_2(PR_3)(\eta^6\text{-}p\text{-cymene})] \quad (3)$$

With a view to further enhance understanding of the formation of bidentate phosphine ruthenium(II)−η^6-arene complexes, we have prepared a range of pendent phosphine complexes of the type [RuCl(PPh_3)(η^1-(P−P))(η^6-*p*-cymene)]PF_6 (P−P = dppm, dppv, dppe, dppp, dppf) and studied the formation of chelate complexes from these cationic precursors and those of the neutral pendent phosphine complexes [$RuCl_2$(η^1-(P−P))(η^6-*p*-cymene)] (P−P = dppm,[9] dppv[10]), for comparison purposes.

Results and Discussion

1. Synthesis and Characterization. Substitution of the labile acetonitrile ligand in [RuCl(CH_3CN)(PPh_3)(η^6-*p*-cymene)]PF_6, **1**, with diphosphine in CH_2Cl_2 at room temperature affords the pendent phosphine complexes [RuCl(PPh_3)(η^1-(P−P))(η^6-*p*-cymene)]PF_6, **[2]PF_6** (P−P = dppm, **a**; dppv, **b**; dppe, **c**; dppp, **d**; dppf, **e**), in high yield, with the exception of **[2e]PF_6**, which is obtained in only moderate yield following recrystallization (ca. 35%), owing to chelation occurring during the course of the reaction and workup (Scheme 1). Small amounts of dimeric species, where the diphosphine bridges two metal centers, can also be observed by ESI-MS and ^{31}P NMR spectroscopy during the preparation of **[2d]PF_6**. This impurity is readily removed by recrystallization, and such dimeric species are not observed for the other reactions, presumably owing to the reluctance of the phosphine to bridge two charged centers, in marked contrast to similar reactions of diphosphines with [$RuCl_2$(η^6-*p*-cymene)]$_2$.[10]

The pendent coordination mode of the diphosphine is clearly evidenced by ^{31}P NMR spectroscopy, where, typically, three distinct resonances are observed, with large $^2J_{PP}$ couplings (ca. 50 Hz) between the coordinated phosphorus centers.[11] The resonance corresponding to the pendent center is in each case

Scheme 1

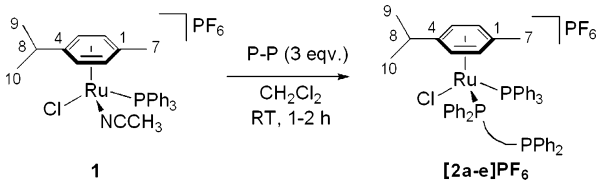

1 **[2a-e]PF_6**

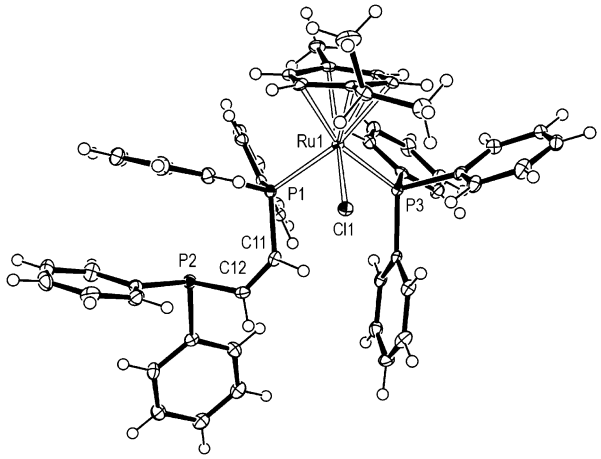

Figure 1. ORTEP representation of **[2b]PF_6**; thermal ellipsoids are drawn at the 50% probability level. Counterion is omitted for clarity. Relevant bond parameters are given in Table 2.

Table 2. Key Bond Lengths (Å) and Angles (deg) for [2a]PF_6, [2b]PF_6, and [2d]PF_6

	[2a]PF_6	[2b]PF_6	[2d]PF_6
Ru1−Cl1	2.394(2)	2.3907(9)	2.401(2)
Ru1−P1	2.393(2)	2.3756 (11)	2.393(2)
Ru1−P3	2.373(2)	2.3811(9)	2.359(2)
Ru1−C1	2.281(7)	2.328(3)	2.293(6)
Ru1−C4	2.333(6)	2.345(3)	2.342(5)
Ru1−C_{avg}	2.27(4)	2.28(5)	2.28(4)
Cl1−Ru1−P1	87.95(6)	86.49(4)	88.29(6)
Cl1−Ru1−P3	85.69(5)	87.73(3)	88.04(5)
P1−Ru1−P3	94.28(6)	93.77(4)	93.97(5)

located at lower frequency, and for **[2a−c]PF_6**, J_{PP} couplings are observed between the diphosphine centers. The ^{1}H and ^{13}C NMR spectra also corroborate the structures well; relevant NMR data for **1** and **[2a−e]PF_6** are compiled in Table 1.

The X-ray structures of **[2a]PF_6** (Figure S2), **[2b]PF_6** (Figure 1), and **[2d]PF_6** (Figure S3) exhibit the typical "piano-stool" geometry around the ruthenium and have generally comparable structural parameters to the related complex [RuCl(PPh_3)$_2$(η^6-*p*-cymene)]BF_4 (**3**),[12] although the P−Ru−P angles are significantly reduced in comparison, i.e., **[2a]PF_6** 94.28(6)°, **[2b]PF_6** 93.77(4)°, **[2d]PF_6** 93.97(5)°, **3** 97.97(2)°. In each case, the Ru−C4 distances are elongated, in comparison to the other arene

(9) Coleman, A. W.; Jones, D. F.; Dixneuf, P. H.; Brisson, C.; Bonnet, J.-J.; Lavigne, G. *Inorg. Chem.* **1984**, *23*, 952−956.
(10) Chaplin, A. B.; Scopelliti, R.; Dyson, P. J. *Eur. J. Inorg. Chem.* **2005**, 4762−4774.
(11) For **[2c]PF_6**, the coordinated phosphorus resonances are non-first-order and are instead observed as a multiplet between 22.0 and 23.7 ppm; see Figure S1.
(12) Lalremputa, R.; Carroll, P. J.; Kollipara, M. R. *J. Coord. Chem.* **2003**, *56*, 1499−1504.

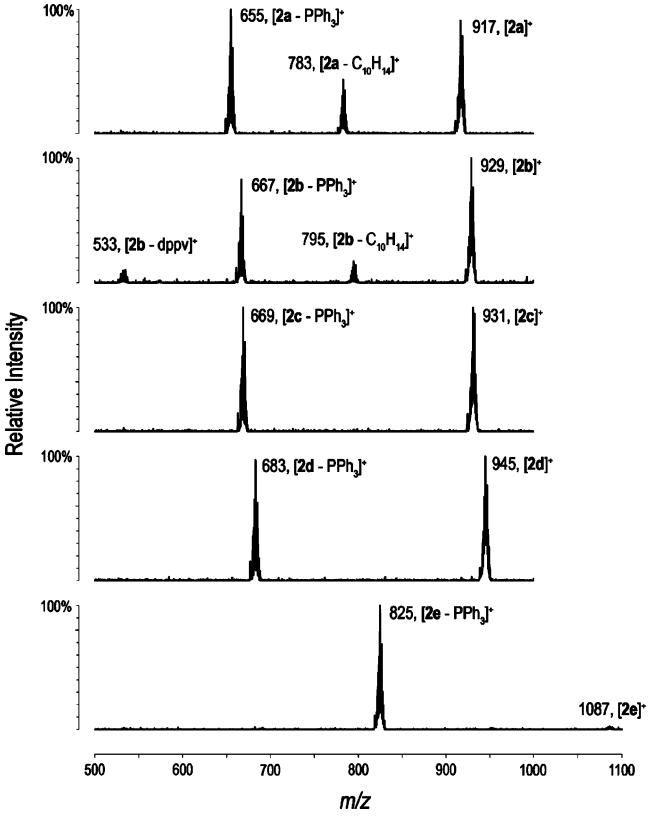

Figure 2. ESI-MS^2 of complexes **[2a−e]PF$_6$** (CH_2Cl_2, 50 °C, 19% normalized collision energy).

Scheme 2. Chelation of Complexes 4a and 4b

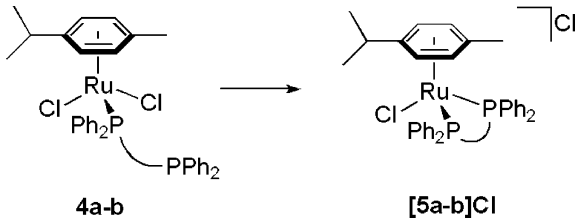

4a-b **[5a-b]Cl**

atoms, consistent with the solution ^{13}C NMR data.[13] The Ru−C1 distance is also elongated in the dppv complex, **[2b]PF$_6$**, suggesting more constrained bonding, and this hypothesis is supported by reduced intramolecular contacts between the two phosphines [P3···C11 = 4.038(7) Å in **[2a]PF$_6$**; 3.865(3) Å in **[2b]PF$_6$**; 4.021(7) Å in **[2d]PF$_6$**].

The ESI-MS of **1** and **[2a−e]PF$_6$** display the desired parent ions, together with peaks of lower relative intensity resulting from loss of either CH_3CN or phosphine ligand, respectively. Of these, the peak resulting from loss of CH_3CN is the most significant, with a relative intensity of 55%, consistent with the labile nature of this ligand, whereas those resulting from loss of PPh_3 have relative intensities of ca. 20%. In the spectra of **[2b]**$^+$ and **[2e]**$^+$, loss of the diphosphine is also observed, with relative intensities of 15% and 11%, respectively. To further

(13) Considerable shifts to higher frequency are observed for the C^4 resonance (see Scheme 1 for labeling) on substitution of the CH_3CN, indicative of weaker coordination of C^4 to the metal center due to increased steric bulk in the coordination sphere. The increase in steric bulk is also apparent from changes in the *p*-cymene H^7 and H^8 resonances and the H^9 and H^{10} resonances, which become distinctly diastereotopic for **[2a−e]PF$_6$**, particularly for **[2b]PF$_6$** and **[2e]PF$_6$**. In the case of **[2e]PF$_6$**, the observation of a NOE interaction between H^6 and H^{12} (Experimental Section, Figure 6), indicating that the dppf ligand adopts a conformation with the ferrocene moiety approaching the plane of the coordinated arene, may help explain the origin of these shifts.

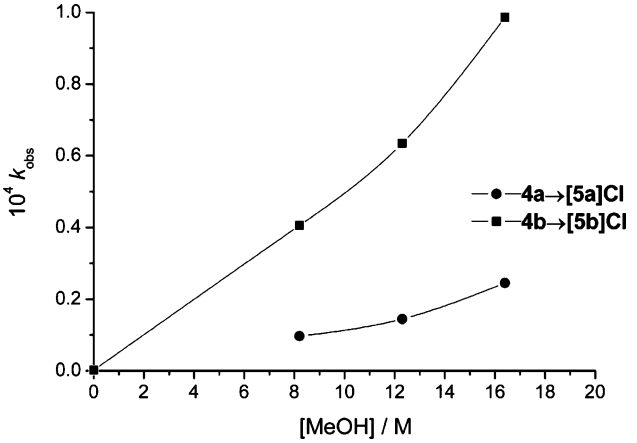

Figure 3. Effect of MeOH concentration on the chelation of complexes **4a** and **4b** in 1,2-dichlorethane at 298 K (data for the chelation of **4b** at [MeOH] = 0 is extrapolated from higher temperature data).

investigate the stability of complexes **[2a−e]**$^+$, to supplement the discussion of the chelation kinetics (see below), selective fragmentation of the parent peak was carried out (ESI-MS^2), Figure 2. Loss of PPh_3 is found to be the primary fragmentation path for these complexes and occurs to approximately the same extent for each complex with the exception of **[2e]**$^+$, where it occurs much more readily, suggesting that it is more weakly coordinated in this complex. Additionally, loss of the arene occurs for **[2a]**$^+$ and **[2b]**$^+$, notably more for the dppm complex, but to a significantly lower extent than PPh_3 loss. Some diphosphine loss can be detected for **[2b]**$^+$, but it is a comparably minor fragmentation pathway.

2. Chelation Kinetics. The neutral pendent phosphine complexes [$RuCl_2$(η^1-(P−P))(η^6-*p*-cymene)] (P−P = dppm, **4a**; dppv, **4b**) readily form ionic chelate complexes via ring closure of the pendent phosphine moiety in 1,2-dichloroethane (or CH_2Cl_2)−MeOH solutions; see Scheme 2. In the absence of MeOH, this process is almost suppressed for complex **4a** (**4a**: **[5a]**$^+$ ≈ 1:0.05 after 7 days in CH_2ClCH_2Cl at 293 K), while greatly reduced for **4b**. To quantify these observations, a kinetic study of the influence of the MeOH concentration on the rate of chelation was carried out in 1,2-dichloroethane by following the changes in the ^{31}P NMR spectra over time. The results from these experiments, depicted in Figure 3, confirm the large influence of methanol on the ring-closure process (related data are also listed in Table 3). Arena and co-workers observed a similar trend for the chelation reactions of complexes of formula [$RuCl_2$(η^6-arene)(P−N*)] (P−N* = P-bound enantiomerically pure (β-aminoalkyl)phosphine) in chloroform, with the observed rate and MeOH concentration linearly correlated.[14] This correlation was ascribed to a bimolecular solvolysis involving initial substitution of one Cl^- ligand by a MeOH molecule followed by ring closure. Accordingly, decreases in the reaction rate were observed on the addition of excess chloride. In contrast, the addition of excess [NMe_4]Cl (20 equiv) does not inhibit the observed rate of chelation for **4a** and **4b** and there is no significant linear correlation between the observed rate and the MeOH concentration. Furthermore, no decreases are found if the reactions are carried out with a large excess of CH_3CN, a more strongly coordinating solvent. Together, these results suggest that the ring-closing process for complexes **4a** and **4b** does not occur via dissociative substitution. The significant role

(14) Arena, C. G.; Calamia, S.; Farone, F.; Graiff, C.; Tiripicchio, A. *J. Chem. Soc., Dalton Trans.* **2000**, 3149−3157.

Table 3. Rate of Chelation for 4a and 4b in Different Solvent Mixtures at 298 K

	ligand	solvent (v/v)	$10^4 k_{obs}/s^{-1}$ (298 K)[a]	$t_{1/2}$ (298 K)[b]
4a → [5a]Cl	dppm	2:1 MeOH−CH_2ClCH_2Cl	0.25	47 min
		1:1 MeOH−CH_2ClCH_2Cl	0.14	80 min
		1:2 MeOH−CH_2ClCH_2Cl	0.097	120 min
		1:1:1 MeOH−CH_2ClCH_2Cl−CH_3CN	0.11	100 min
		1:1:1 MeOH−CH_2ClCH_2Cl−DMSO	0.026	440 min
		1:1 MeOH−CH_2ClCH_2Cl + $[NMe_4]Cl$[c]	0.15	77 min
4b → [5b]Cl	dppv	2:1 MeOH−CH_2ClCH_2Cl	0.99	12 min
		1:1 MeOH−CH_2ClCH_2Cl	0.64	18 min
		1:2 MeOH−CH_2ClCH_2Cl	0.41	28 min
		CH_2ClCH_2Cl	0.002[d]	4 days[d]
		1:1:1 MeOH−CH_2ClCH_2Cl−CH_3CN	0.43	27 min
		1:1:1 MeOH−CH_2ClCH_2Cl−DMSO	0.11	100 min
		1:1 MeOH−CH_2ClCH_2Cl + $[NMe_4]Cl$[c]	0.82	14 min

[a] Errors were typically ±5%. [b] $t_{1/2}$ (ln(2)/k_{obs}) values included for ease of comparison. [c] 20 equiv per complex. [d] Extrapolated from higher temperature data.

Table 4. Activation Parameters for the Chelation of Complexes 4a and 4b

	ligand	solvent	$\Delta H^{\ddagger}$/kJ mol^{-1}	$\Delta S^{\ddagger}$/J mol^{-1}K^{-1}	$\Delta V^{\ddagger}$/cm^3 mol^{-1} (298 K)
4a → [5a]Cl	dppm	1:1 MeOH−CH_2ClCH_2Cl	92.7 ± 1.0	−7 ± 3	+2.7 ± 0.3
4b → [5b]Cl	dppv	1:1 MeOH−CH_2ClCH_2Cl	79 ± 2	−41 ± 5	−4.0 ± 0.5
4b → [5b]Cl	dppv	CH_2ClCH_2Cl	97 ± 2	−29 ± 7	

of the MeOH in this process may be attributed to the formation of hydrogen bonds with the chloride ligands, which serve to stabilize the loss of chloride, consistent with the observation that the addition of DMSO, a good H-bond acceptor,[15] significantly decreases the rate of chelation for both complexes **4a** and **4b**. In all cases the chelation proceeded smoothly and no side products or intermediates were observed by ^{31}P NMR spectroscopy.

The chelation of **4b** can also be effected in 1,2-dichloroethane at elevated temperatures, although accompanied by the formation of significant amounts of *trans*-[$RuCl_2$(η^2-dppv)$_2$], identified by a resonance at 53.6 ppm in ^{31}P NMR spectra.[16] Another minor product is also observed with a resonance at 84.4 ppm and possibly corresponds to a higher nuclearity, chloride-bridged, species owing to the similarity of the chemical shift with related 1,2-bis(diphenylphosphino)benzene complexes, prepared from η^2-diphosphine ruthenium−arene complexes.[17] Under comparable conditions, an authentic sample of **[5b]Cl** showed no significant decomposition, indicating that these two side products are likely to originate from arene loss, rather than chloride loss, during the ring-closing reaction. This alternative reaction pathway seems to be dominant in 1,2-dichloroethane for **4a**, as heating does not result in the formation of **[5a]**$^+$, but primarily in *trans*-[$RuCl_2$(η^2-dppm)$_2$][18] and [$RuCl_2$(η^6-*p*-cymene)]$_2$(μ-dppm).[19] Such a difference is consistent with the observed fragmentation patterns of **[2a]**$^+$ and **[2b]**$^+$ (Figure 2), with the dppm complex showing a larger tendency for arene loss.

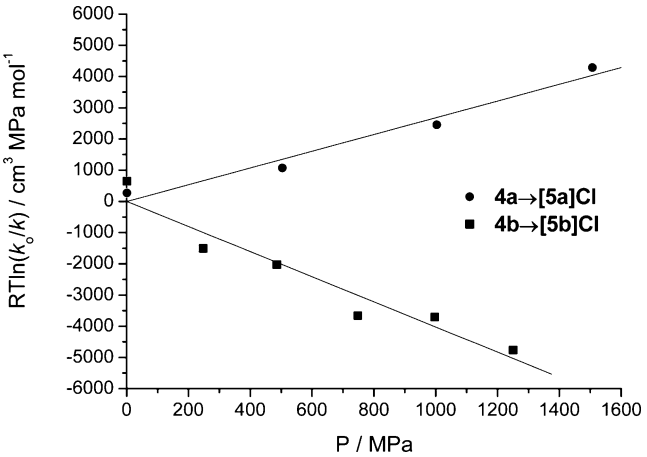

Figure 4. Pressure dependence for the chelation of complexes **4a** (R^2 = 0.971) and **4b** (R^2 = 0.933) in 1:1 MeOH−CH_2ClCH_2Cl at 298 K determined by high-pressure UV−visible spectroscopy.

Activation enthalpies and entropies for the chelation reactions of **4a** and **4b** in 1:1 MeOH−1,2-dichloroethane (by following the consumption of **4a** or **4b**) and **4b** in 1,2-dichloroethane (by following the formation of **[5b]**$^+$) have been determined by ^{31}P NMR spectroscopy, and additionally, the volumes of activation for the former have been determined using variable-pressure UV−visible spectroscopy; the results of these studies are compiled in Table 4, with the pressure dependence depicted in Figure 4. Together these activation parameter values are consistent with a concerted substitution of chloride during the ring-closure process. Complex **4a** seems to react with a more dissociative character owing to the more positive $\Delta S^{\ddagger}$ value and positive $\Delta V^{\ddagger}$ value, whereas **4b** reacts with a higher degree of associative character.[20] This difference in reactivity is also implied by the large difference in the chelate bite angles in these complexes [**[5a]BF$_4$**, 71.29(6)°;[4] **[5b]PF$_6$**, 83.46(3)°, 83.39(3)°], with the larger bite angle of the dppv ligand more closely resembling that of the nonchelating bite angle of 97.7° in **3**.[12] The activation parameters determined for **4b** are comparable

(15) Abraham, M. H. *Chem. Soc. Rev.* **1993**, 73−83.
(16) Batista, A. A.; Cordeiro, L. A. C.; Olvia, G.; Nascimento, O. R. *Inorg. Chim. Acta* **1997**, *258*, 131−137.
(17) (a) Mashima, K.; Komura. N.; Yamagata, T.; Tani, K.; Haga, M.-A. *Inorg. Chem.* **1997**, *36*, 2908−2912. (b) Mashima, K.; Nakamura, T.; Matsuo, Y.; Tani, K. *J. Organomet. Chem.* **2000**, *607*, 51−56.
(18) Jung, C. W.; Garrou, P. E.; Hoffman, P. R.; Caulton, K. G. *Inorg. Chem.* **1984**, *23*, 726−729.
(19) Estevan, F.; Lahuerta, P.; Latorre, J.; Sanchez, A.; Sieiro, C. *Polyhedron* **1987**, *6*, 473−478.
(20) The overall volume of activation is comprised of both intrinsic and solvational contributions ($\Delta V^{\ddagger}_{obs} = \Delta V^{\ddagger}_{intr} + \Delta V^{\ddagger}_{solv}$). Because the chelation of **4a** and **4b** involves the creation of charged species (**[5a]**$^+$**Cl**$^-$, **[5b]**$^+$**Cl**$^-$, respectively), the overall volume of activation value will include a negative contribution from changes in the solvation during this process (electrostriction), making the precise interpretation of the overall volume of activation less straightforward [van Eldik, R.; Hubbard, C. D. *High Pressure Chemistry*; van Eldik, R., Klärner, F.-G., Eds.; Wiley-VCH: Weinhein, 2002]. However, owing to the similarity of these two complexes, contributions from electrostriction are likely to be similar. In addition to the volumes of activation, similar arguments apply to the interpretation of the activation entropies for the chelation of **4a** and **4b**. The electrostriction is likely to be negligable in the chelation of **[2a−e]PF$_6$**, as there is no change in charge, and furthermore 1,2-dichloroethane is an apolar solvent (electrostriction during the chelation of **4b** in 1,2-dichloroethane could also be expected to be small).

Table 5. Activation Parameters for the Chelation of Complexes [2a−e]PF_6 in 1,2-Dichloroethane

	ligand	$\Delta H^{\ddagger}$/kJ mol^{-1}	$\Delta S^{\ddagger}$/J mol^{-1} K^{-1}	$10^4 k_{obs}$/s^{-1} (353 K)[a]	$t_{1/2}$ (353 K),[b] min
[2a]PF_6 → **[5a]PF_6**[c]	dppm	118 ± 3	23 ± 8	3.8	30
[2b]PF_6 → **[5b]PF_6**[d]	dppv	119 ± 3	25 ± 10	3.8	30
[2c]PF_6 → **[5c]PF_6**	dppe	136 ± 5	74 ± 15	4.1	28
[2d]PF_6 → **[5d]PF_6**	dppp	132 ± 2	66 ± 5	5.2	22
[2e]PF_6 → **[5e]PF_6**[e]	dppf	126 ± 4	77 ± 12	160	1

[a] Calculated from fit to Eyring equation. [b] $t_{1/2}$ (ln(2)/k_{obs}) values included for ease of comparison. [c] Side products: [$RuCl_2(PPh_3)$(dppm)$_2$], [$RuCl(PPh_3)_2(\eta^6$-*p*-cymene)]$^+$. [d] Side products: [$RuCl_2$(dppv)$_2$], [$RuCl(PPh_3)_2(\eta^6$-*p*-cymene)]$^+$. [e] Side product: [$RuCl(PPh_3)_2(\eta^6$-*p*-cymene)]$^+$.

Scheme 3. Preparation of 5b

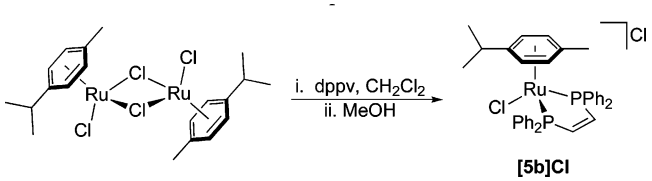

Scheme 4. Chelation of Complexes [2a−e]PF_6

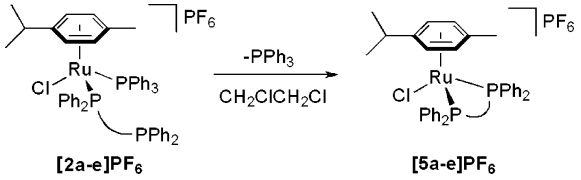

to those reported for the chelation of [$RuCl_2(\eta^6$-*p*-cymene)(*S*-phephos)][7] in $CHCl_3$−MeOH ($\Delta H^{\ddagger}$ = 75.66 kJ mol^{-1}, $\Delta S^{\ddagger}$ = −48.07 J mol^{-1} K^{-1}).[14]

Following the investigation of the chelation process, a one-pot, high-yielding synthesis of **[5b]Cl** was developed and is shown in Scheme 3. Via this method, the pendent phosphine complex **4b** is prepared from the reaction between [$RuCl_2(\eta^6$-*p*-cymene)]$_2$ and dppv in CH_2Cl_2 and the ring closure effected by the addition of MeOH, giving **[5b]Cl** in 99% yield. The corresponding PF_6 salt is readily obtained by metathesis in MeOH using [NH_4]PF_6, and its solid-state structure determined by X-ray diffraction is depicted in Figure 5.

Complexes **[2a−e]PF_6** also undergo ring-closing reactions on heating in 1,2-dichloroethane, with the loss of PPh_3, leading to the formation of chelating compounds **[5a−e]PF_6**; see Scheme 4. In each case, this process is the primary reaction pathway for the complexes and concurs with the ESI-MS data, which indicated that PPh_3 is the most labile ligand in these complexes. Formation of [$RuCl(PPh_3)_2(\eta^6$-*p*-cymene)]$^+$, **6**,[12] is observed during the reactions of **[2a]PF_6**, **[2e]PF_6**, and, most significantly, **[2b]PF_6**, most probably owing to a large degree of steric pressure in the coordination sphere of these complexes

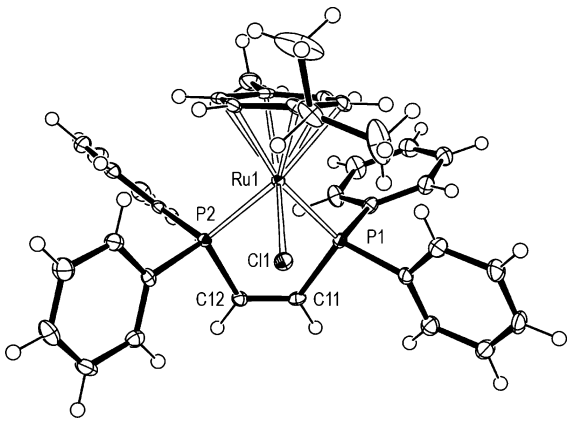

Figure 5. ORTEP representation of **[5b]PF_6**, one of the two molecular units in the asymmetric cell. Thermal ellipsoids are drawn at the 50% probability level. Counterion and solvent molecule are omitted for clarity. Key bond lengths (Å) and angles (deg), equivalent parameters from the other unit in brackets: Ru1−Cl1, 2.3978(7) {2.3936(7)}; Ru1−P1, 2.3172(8) {2.3205(8)}; Ru1−P2, 2.3240(7) {2.3133(8)}; Ru1−C1, 2.284(3) {2.276(2)}; Ru1−C4, 2.312(3) {2.308(2)}; Ru1−C_{av}, 2.27(3) {2.27(3)}; Cl1−Ru1−P1, 84.68(3) {84.70(3)}; Cl1−Ru1−P2, 82.92(3) {82.99(3)}; P1−Ru1−P2, 83.46(3) {83.39(3)}.

(**6**:**[5a]**$^+$ ≈ 1:41; **6**:**[5b]**$^+$ ≈ 1:4; **6**:**[5e]**$^+$ ≈ 1:13 at 333 K near reaction completion).[13] Additionally, arene loss is observed during the reactions of **[2a]PF_6** and **[2b]PF_6**, as indicated by a distinctive ABX pattern, which may be assigned to [$RuCl_2(PPh_3)(\eta^2$-dppm)] (**7**),[21] and signals corresponding presence of *cis*- and *trans*-[$RuCl_2(\eta^2$-dppv)$_2$] (**8**)[16] in the ^{31}P NMR spectra, respectively. This pathway is significantly more favored for the dppm complex than that of the dppv complex (**7**:**[5a]**$^+$ ≈ 1:3; **8**:**[5b]**$^+$ ≈ 1:5 at 333 K near reaction completion), matching the previous trend observed for the corresponding reactions of **4a** and **4b** in 1,2-dichloroethane and the ESI-MS data, shown in Figure 2. Complexes **[2c]PF_6** and **[2d]PF_6** react smoothly to form the corresponding chelate complexes, **[5c]PF_6** and **[5d]PF_6**, with high selectivity.

Activation parameters for the chelation of **[2a−e]PF_6** in 1,2-dichloroethane have been determined by following the formation of complexes **[5a−e]**$^+$ by ^{31}P NMR spectroscopy and are summarized in Table 5. A precise comparison to those of the chelation reactions of **4a** and **4b** is not possible owing to electrostriction of the solvent during these reactions, originating from the creation of charged species in solution,[20] although the large positive $\Delta S^{\ddagger}$ values characteristic of the chelation reactions of **[2a−e]PF_6** are clearly indicative of a large degree of dissociation during this process in comparison to the concerted process proposed for the neutral compounds.[22] The magnitude of the activation enthalpies is also consistent with a rate-limiting step involving dissociation of PPh_3.[23] The $\Delta S^{\ddagger}$ values for the reactions of complexes **[2a]PF_6** and **[2b]PF_6** are lower in magnitude than the other cationic complexes, perhaps indicating a more concerted chelation process. The formation of the chelate complex of dppf, **[5e]PF_6**, is much more rapid than the other cationic phosphine complexes studied in this investigation, showing an appreciable rate at room temperature ($t_{1/2}$ = 1.6 days at 298 K, extrapolated). The origin of this marked difference may stem from the bulky nature of the dppf ligand, weakening the Ru−PPh_3 bond. ESI-MS^2 of **[2e]**$^+$ is consistent

(21) ^{31}P{^{1}H} NMR (CH_2ClCH_2Cl, internal D_2O reference): δ 38.8 (t, $^2J_{PP}$ = 34, 1P, *P*Ph_3), 5.6 (dd, $^2J_{PP}$ = 69, $^2J_{PP}$ = 34, 1P, *P*Ph_2), 4.7 (dd, $^2J_{PP}$ = 69, $^2J_{PP}$ = 34, 1P, *P*′Ph_2). The analogous compounds [$RuCl_2(PPh_3)(\eta^2$-(P−P))] (P−P = dppp, dppb) have been reported and exhibit similar ^{31}P NMR spectra, although with larger $J_{(P-P)(P-P)}$ coupling constants [ref 18].

(22) Since electrostriction effects are likely to be minimal in 1,2-dichloroethane, a comparison between the chelation reactions of the charged, **[2b]PF_6**, and neutral, **4b**, pendant complexes is likely to be reliable. Hence, the large difference in magnitude and different sign of the $\Delta S^{\ddagger}$ values for these complexes supports the mechanistic hypotheses.

(23) Dias, P. B.; Minas de Piedade, M. E.; Simões, J. A. M. *Coord. Chem. Rev.* **1994**, *135*−*136*, 737−807.

Scheme 5. Schematic Representation of Proposed Transition States for the Chelation Reactions

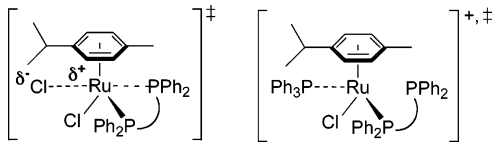

with this hypothesis, showing the facile loss of PPh_3 in comparison to **[2a−d]**$^+$. Both $\Delta H^‡$ and $\Delta S^‡$ values for the chelation reactions of the dppm, dppe, and dppp complexes are significantly larger than those of the corresponding complexes involving substitution of CO: [Ru(CO)$_4$(η^1-(P−P))] (P−P [$\Delta H^‡$/kJ mol^{-1}, $\Delta S^‡$/J mol^{-1} K^{-1}] = dppm [105 ± 3, 13 ± 5], dppe [107.5 ± 1.3, 13 ± 6], dppp [109.2 ± 1.3, 21 ± 4]).[6]

Conclusions

The chelation kinetics of a series of ruthenium(II)−η^6-*p*-cymene phosphine complexes have been studied. Neutral complexes of general formula [RuCl$_2$(η^1-(P−P))(η^6-*p*-cymene)] (P−P = dppm, **4a**; dppv, **4b**) readily form chelate complexes, [RuCl(η^2-(P−P))(η^6-*p*-cymene)]Cl, in the presence of MeOH, which assists the ring-closing process by formation of hydrogen bonds with the chloride ligands, thereby facilitating their activation. In the absence of such interactions the process is much slower, requiring elevated temperatures, and arene loss becomes increasingly dominant. On the basis of entropies, enthalpies, and volumes of activation, a concerted chloride substitution mechanism is proposed, as illustrated in Scheme 5. Related cationic complexes of formula [RuCl(PPh$_3$)(η^1-(P−P))(η^6-*p*-cymene)]PF$_6$, **2** (P−P = dppm, **a**; dppv, **b**; dppe, **c**; dppp, **d**; dppf, **e**) also form chelate complexes, [RuCl(η^2-(P−P))(η^6-*p*-cymene)]PF$_6$, via a dissociative mechanism involving loss of PPh_3. However, elevated temperatures are generally required and a number of alternative reaction pathways can be observed for complexes **[2a]PF$_6$**, **[2b]PF$_6$**, and **[2e]PF$_6$**, albeit of secondary importance. Notably, ESI-MS of complexes **[2a−e]PF$_6$** has provided not only useful structural information but also a number of insights in the reactivity, supplementing the kinetic investigations well.

Experimental Section

All organometallic manipulations were carried out under a nitrogen atmosphere using standard Schlenk techniques. CH_2Cl_2 was dried catalytically under dinitrogen using a solvent purification system, manufactured by Innovative Technology Inc. 1,2-Dichloroethane was distilled from P_2O_5 under dinitrogen. All other solvents were p.a. quality. [RuCl$_2$(η^6-*p*-cymene)]$_2$,[24] [RuCl$_2$(PPh$_3$)(η^6-*p*-cymene)],[25] [RuCl$_2$(η^1-dppm)(η^6-*p*-cymene)],[4d] and [RuCl$_2$(η^1-dppv)(η^6-*p*-cymene)][10] were prepared as described elsewhere. All other chemicals are commercial products and were used as received. NMR spectra were recorded with a Bruker Avance 400 spectrometer at room temperature, unless otherwise stated. Chemical shifts are given in ppm and coupling constants (*J*) in Hz. Simulation analysis of the ^{31}P NMR spectra of **[2c]PF$_6$** was carried out using g-NMR.[26] ESI-MS were recorded on a Thermo Finnigan LCQ DECA XPPlus, using a literature protocol,[27] and microanalyses performed at the EPFL. Labeling schemes for the NMR data are indicated in Scheme 1 (labels for the carbon atoms of ligands increase from the coordinated atom, excluding the Ph groups) and Figure 6.

Preparation of [RuCl(CH$_3$CN)(PPh$_3$)(η^6-*p*-cymene)]PF$_6$. A suspension of [RuCl$_2$(PPh$_3$)(η^6-*p*-cymene)] (1.30 g, 2.29 mmol) and [NH$_4$]PF$_6$ (0.49 g, 2.98 mmol) in CH_3CN (70 mL) was heated at reflux for 10 min. The solvent was then removed and the residue extracted with CH_2Cl_2 through Celite. The product was precipitated as an oil by the addition of pentane, the supernatant removed by decantation, and then sonicated twice in pentane and then diethyl ether. Yield: 1.43 g (87%) as a yellow powder. ^{1}H NMR ($CDCl_3$): δ 7.45−7.70 (m, 15H, P*Ph*$_3$), 6.13 (d, $^3J_{HH}$ = 5.6, 1H, H^5), 5.94 (d, $^3J_{HH}$ = 5.6, 1H, H^3), 5.41 (d, $^3J_{HH}$ = 5.6, 1H, H$_2$), 4.66 (d, $^3J_{HH}$ = 5.5, 1H, H^6), 3.05 (sept, $^3J_{HH}$ = 6.7, 1H, H^8), 1.95 (s, 3H, H^{12}), 1.75 (s, 3H, H^7), 1.38 (d, $^3J_{HH}$ = 7, 3H, H^9), 1.36 (d, $^3J_{HH}$ = 7, 3H, H^{10}). ^{13}C{^{1}H} NMR ($CDCl_3$): δ 134.5 (d, $^2J_{PC}$ = 10, P*Ph*$_3$), 131.4 (d, $^4J_{PC}$ = 3, P*Ph*$_3$), 130.0 (d, $^1J_{PC}$ = 49, P*Ph*$_3$), 128.6 (d, $^3J_{PC}$ = 11, P*Ph*$_3$), 127.4 (s, C^{11}), 116.6 (d, $^2J_{PC}$ = 8, C^4), 103.6 (s, C^1), 95.6 (d, $^2J_{PC}$ = 6, C^3), 89.7 (s, C^6), 89.2 (br, C^5), 85.0 (br, C^2), 31.2 (s, C^8), 23.6 (s, C^{10}), 21.2 (s, C^9), 18.3 (s, C^7), 3.2 (s, C^{12}). ^{31}P{^{1}H} NMR ($CDCl_3$): δ 35.5 (s, 1P, Ru*P*Ph$_3$), −144.1 (sept, $^1J_{PF}$ = 713, 1P, *P*F$_6$). ESI-MS (CH_2Cl_2) positive ion: *m/z*, 533 (55%) [M − CH_3CN]$^+$, 574 [M]$^+$; negative ion: *m/z*, 145 [PF$_6$]$^-$. Anal. Calcd for $C_{30}H_{32}ClF_6NP_2Ru$ (719.05 g mol^{-1}): C, 50.11; H, 4.49; N, 1.95. Found: C, 50.32; H, 4.55; N, 1.95.

Preparation of [RuCl(PPh$_3$)(η^1-P−P)(η^6-*p*-cymene)]PF$_6$: General Procedure. A solution of [RuCl(CH$_3$CN)(PPh$_3$)(η^6-*p*-cymene)]-PF$_6$ (0.50 g, 0.70 mmol) and diphosphine (3 equiv, 2.1 mmol) in CH_2Cl_2 (20 mL) was stirred at RT for 1−2 h. The product was then precipitated by the addition of excess diethyl ether (100 mL), washed with ether (3 × 50 mL), and dried in vacuo. Further purification, if necessary, was achieved by recrystallization from CH_2Cl_2−pentane.

[RuCl(PPh$_3$)(η^1-dppm)(η^6-*p*-cymene)]PF$_6$. Yield: 0.67 g (90%) as a microcrystalline yellow-orange solid. Orange crystals suitable for X-ray diffraction were obtained by recrystallization from CH_2Cl_2−pentane. ^{1}H NMR ($CDCl_3$): δ 6.9−7.9 (m, 35H, P*Ph*), 5.93 (dd, $^3J_{HH}$ = 6.2, $^3J_{PH}$ = 4, 1H, H^6), 5.66 (d, $^3J_{HH}$ = 6.1, 1H, H^3), 5.25 (dd, $^3J_{HH}$ = 6.4, $^3J_{PH}$ = 4, 1H, H^2), 4.95 (d, $^3J_{HH}$ = 6.0, 1H, H^5), 3.68 (ddd, $^2J_{HH}$ = 16.1, $^2J_{PH}$ = 6.5, $^2J_{PH}$ = 2, 1H, H^{11}), 2.78 (sept, $^3J_{HH}$ = 6.9, 1H, H^8), 1.31 (d, $^3J_{HH}$ = 6.9, 3H, H^9), 1.25 (d, $^3J_{HH}$ = 6.9, 3H, H^{10}), 0.95 (obscured, 1H, H$^{11'}$), 0.93 (s, 3H, H^7). ^{13}C{^{1}H} NMR ($CDCl_3$): δ 127.5−134.5 (m, P*Ph*), 132 (C^4), 99.3 (d, $^2J_{PC}$ = 3, C^2), 98.7 (s, C^1), 95.6 (d, $^2J_{PC}$ = 3, C^6), 90.1 (d, $^2J_{PC}$ = 10, C^5), 87.2 (d, $^2J_{PC}$ = 10, C^3), 31.7 (s, C^8), 21.5 (s, C$^{9/10}$), 21.3 (s, C$^{10/9}$), 18.9 (dd, $^1J_{PC}$ = 33,$^1J_{PC}$ = 26, C^{11}), 15.1 (s, C^7). ^{31}P{^{1}H} NMR ($CDCl_3$): δ 23.0 (d, $^2J_{PP}$ = 52, 1P, Ru-*P*Ph$_3$), 22.0 (dd, $^2J_{PP}$ = 52, $^2J_{PP}$ = 44, 1P, Ru-*P*Ph$_2$), −28.8 (d, $^2J_{PP}$ = 43.7, 1P, *pend*-*P*Ph$_2$), −144.4 (sept, $^1J_{PF}$ = 713, 1P, *P*F$_6$). ESI-MS (CH_2Cl_2) positive ion: *m/z*, 655 (18%) [M − PPh$_3$]$^+$, 917 [M]$^+$; negative ion: *m/z*, 145 [PF$_6$]$^-$. Anal. Calcd for $C_{53}H_{51}ClF_6P_4Ru$ (1062.40 g mol^{-1})·$^3/_4CH_2Cl_2$: C, 57.33; H, 4.70. Found: C, 57.13; H, 4.53.

[RuCl(PPh$_3$)(η^1-dppv)(η^6-*p*-cymene)]PF$_6$. Yield: 0.53 g (71%) as a yellow powder. Orange crystals suitable for X-ray diffraction were obtained by slow diffusion of diethyl ether into a CH_2Cl_2 solution of the compound at RT. ^{1}H NMR ($CDCl_3$): δ 7.91−8.03 (m, 2H, RuP*Ph*$_2$), 7.00−7.71 (m, 29H, P*Ph*), 6.93−7.00 (m, 2H, *pend*-P*Ph*$_2$), 6.84 (ddd, $^2J_{PH}$ = 38, $^3J_{HH}$ = 13.7, $^3J_{PH}$ = 4, 1H, H^{11}), 6.53 (ddd, $^2J_{PH}$ = 30, $^2J_{PH}$ = 29, $^3J_{HH}$ = 13.6, 1H, H^{12}), 6.45−6.51 (m, 2H, *pend*-P*Ph*$_2$), 6.11 (dd, $^3J_{HH}$ = 6.1, $^3J_{PH}$ = 5, 1H, H^6), 5.76 (d, $^3J_{HH}$ = 6.2, 1H, H^3), 5.21 (dd, $^3J_{HH}$ = 6.4, $^3J_{PH}$ = 5, 1H, H^2), 4.66 (d, $^3J_{HH}$ = 6.1, 1H, H^5), 2.58 (sept, $^3J_{HH}$ = 6.9, 1H, H^8), 1.30 (d, $^3J_{HH}$ = 7.0, 3H, H^9), 1.11 (d, $^3J_{HH}$ = 6.9, 3H, H^{10}), 0.99 (s, 3H, H^7). ^{13}C{^{1}H} NMR ($CDCl_3$): δ 149.2 (dd, $^1J_{PC}$ = 21, $^2J_{PC}$ = 8, C^{11}), 135.0 (dd, $^1J_{PC}$ = 45, $^2J_{PC}$ = 21, C^{12}), 127−139 (m, P*Ph*), 130 (C^4), 100.6 (s, C^1), 98.8 (d, $^2J_{PC}$ = 5, C^2), 94.0 (d, $^2J_{PC}$ = 2, C^6), 91.2 (d, $^2J_{PC}$ = 9, C^5), 88.7 (d, $^2J_{PC}$ = 10), 31.4 (s, C^8), 21.9

(24) Bennett, M. A.; Huang, T. N.; Matheson, T. W.; Smith, A. K. *Inorg. Synth.* **1982**, *21*, 74−78.
(25) Bennett, M. A.; Smith, A. K. *J. Chem. Soc., Dalton Trans.* **1974**, 233−241.
(26) Budzelaar, P. H. M. *g-NMR* v4.0; IvorySoft, 1997.
(27) Dyson, P. J.; McIndoe, J. S. *Inorg. Chim. Acta* **2003**, *354*, 69−74.

(s, C^9), 21.2 (s, C^{10}), 15.5 (s, C^7). $^{31}P\{^1H\}$ NMR ($CDCl_3$): δ 25.8 (d, $^2J_{PP}$ = 55, 1P, Ru-*P*Ph_3), 7.4 (dd, $^2J_{PP}$ = 54, $^3J_{PP}$ = 15, 1P, Ru-*P*Ph_2), −33.2 (d, $^3J_{PP}$ = 15, 1P, *pend*-*P*Ph_2), −144.2 (sept, $^1J_{PF}$ = 713, 1P, *P*F_6). ESI-MS (CH_2Cl_2) positive ion: *m/z*, 533 (15%) $[M - dppv]^+$, 667 (21%) $[M - PPh_3]^+$, 929 $[M]^+$; negative ion: *m/z*, 145 $[PF_6]^-$. Anal. Calcd for $C_{54}H_{51}ClF_6P_4Ru$ (1074.41 g mol^{-1})·$^1/_2CH_2Cl_2$: C, 58.61; H, 4.69. Found: C, 58.54; H, 4.65.

[RuCl(PPh$_3$)(η^1-dppe)(η^6-*p*-cymene)]PF$_6$. Yield: 0.53 g (71%) as a yellow powder. ^1H NMR ($CDCl_3$): δ 7.1−7.89 (m, 31H, P*Ph*), 6.89−7.1 (m, 4H, *pend*-P*Ph*$_2$), 6.07 (dd, $^3J_{HH}$ = 6.2, $^3J_{PH}$ = 4, 1H, H^6), 5.69 (d, $^3J_{HH}$ = 6.2, 1H, H^3), 5.23 (dd, $^3J_{HH}$ = 6.2, $^3J_{PH}$ = 5, 1H, H^2), 4.83 (d, $^3J_{HH}$ = 6.1, 1H, H^5), 2.76 (sept, $^3J_{HH}$ = 7.0, 1H, H^8), 2.60−2.7 (m, 1H, $H^{12/11}$), 1.38−1.52 (m, 1H, $H^{11/12}$), 1.30 (d, $^3J_{HH}$ = 7.0, 3H, H^9), 1.23 (d, $^3J_{HH}$ = 6.9, 3H, H^{10}), 0.96−1.09 (m, 1H, $H^{11'/12'}$), 0.84 (s, 3H, H^7), 0.70−0.9 (m, 1H, $H^{12'/11'}$). $^{13}C\{^1H\}$ NMR ($CDCl_3$): δ 128−138 (m, P*Ph*), 132 (C^4), 99.2 (br, C^2), 98.8 (s, C^1), 95.5 (br, C^6), 89.9 (d, $^2J_{PC}$ = 9, C^5), 87.0 (d, $^2J_{PC}$ = 9, C^3), 31.6 (s, C^8), 22 ($C^{11/12}$), 21.8 (s, C^9), 21.0 (s, C^{10}), 17 ($C^{12/11}$), 14.9 (s, C^7). $^{31}P\{^1H\}$ NMR ($CDCl_3$): δ 22.0−23.7 (m, 2P, Ru*P*Ph), −13.0 (dd, $^3J_{PP}$ = 27, $^5J_{PP}$ = 6, 1P, *pend*-*P*Ph_2), −144.3 (sept, $^1J_{PF}$ = 713, 1P, *P*F_6). ESI-MS (CH_2Cl_2) positive ion: *m/z*, 669 (24%) $[M - PPh_3]^+$, 931 $[M]^+$; negative ion: *m/z*, 145 $[PF_6]^-$. Anal. Calcd for $C_{54}H_{53}ClF_6P_4Ru$ (1076.42 g mol^{-1}): C, 60.25; H, 4.96. Found: C, 60.65; H, 5.09.

[RuCl(PPh$_3$)(η^1-dppp)(η^6-*p*-cymene)]PF$_6$. Yield: 0.25 g (76%) as a yellow powder. Orange crystals suitable for X-ray diffraction were obtained by recrystallization from CH_2Cl_2−pentane at 4 °C. ^1H NMR ($CDCl_3$): δ 6.9−7.8 (m, 35H, P*Ph*), 6.03 (dd, $^3J_{HH}$ = 6.1, $^3J_{PH}$ = 5, 1H, H^6), 5.67 (d, $^3J_{HH}$ = 6.1, 1H, H^3), 5.25 (dd, $^3J_{HH}$ = 6.0, $^3J_{PH}$ = 5, 1H, H^2), 4.89 (d, $^3J_{HH}$ = 6.0, 1H, H^5), 2.76 (sept, $^3J_{HH}$ = 6.8, 1H, H^8), 2.55−2.69 (m, 1H, H^{11}), 1.5−1.66 (m, 1H, H^{13}), 1.39−1.51 (m, 1H, $H^{11'}$), 1.30 (d, $^3J_{HH}$ = 6.9, 3H, H^9), 1.25 (d, $^3J_{HH}$ = 6.8, 3H, H^{10}), 0.8−0.98 (m, 1H, H^{12}), 0.85 (s, 3H, H^7), 0.59−0.73 (m, 1H, $H^{13'}$), 0.36−0.56 (m, 1H, $H^{12'}$). $^{13}C\{^1H\}$ NMR ($CDCl_3$): δ 128−135 (m, P*Ph*), 132 (C^4), 99 (C^1), 99 (C^2), 95.3 (d, $^2J_{PC}$ = 3, C^6), 89.6 (d, $^2J_{PC}$ = 10, C^5), 87.3 (d, $^2J_{PC}$ = 10, C^3), 31.6 (s, C^8), 29.1 (dd,$^1J_{PC} \approx {}^3J_{PC}$ = 12, C^{13}), 21.8 (dd,$^1J_{PC}$ = 26, $^3J_{PC}$ = 12, C^{11}), 21.8 (s, C^9), 21.0 (s, C^{10}), 19.7 (dd, $^2J_{PC}$ = 19, $^2J_{PC}$ = 9, C^{12}), 14.9 (s, C^7). $^{31}P\{^1H\}$ NMR ($CDCl_3$): δ 23.2 (d, $^2J_{PP}$ = 52, 1P, Ru-*P*Ph_3), 18.4 (d, $^2J_{PP}$ = 52, 1P, Ru-*P*Ph_2), −18.1 (s, 1P, *pend*-*P*Ph_2), −144.3 (sept,$^1J_{PF}$ = 713, 1P, *P*F_6). ESI-MS (CH_2Cl_2) positive ion: *m/z*, 683 (21%) $[M - PPh_3]^+$, 945 $[M]^+$; negative ion: *m/z*, 145 $[PF_6]^-$. Anal. Calcd for $C_{55}H_{55}ClF_6P_4Ru$ (1090.45 g mol^{-1}): C, 60.58; H, 5.08. Found: C, 60.58; H, 5.07.

[RuCl(PPh$_3$)(η^1-dppf)(η^6-*p*-cymene)]PF$_6$. Yield: 0.30 g (35%) as an orange powder following recrystallization from CH_2Cl_2−pentane at −20 °C. ^1H NMR ($CDCl_3$): δ 6.9−7.8 (m, 35H, P*Ph*), 5.61−5.70 (m, 2H, H^2 + H^3), 5.47 (dd, $^3J_{HH}$ = 6.1, $^3J_{PH}$ = 5, 1H, H^6), 4.98 (br, 1H, H^{15}), 4.48 (br, 1H, H^{14}), 4.26 (br, 1H, H^{13}), 4.19 (d, 1H, H^5), 3.94 (br, 1H, $H^{17/20}$), 3.92 (br, 1H, $H^{18/19}$), 3.88 (br, 1H, H^{12}), 3.83 (br, 1H, $H^{19/18}$), 3.74 (br, 1H, $H^{20/17}$), 2.67 (sept, $^3J_{HH}$ = 6.9, 1H, H^8), 1.35 (d, $^3J_{HH}$ = 6.9, 3H, H^9), 1.16 (d, $^3J_{HH}$ = 7.0, 3H, H^{10}), 1.10 (s, 3H, H^7). $^{13}C\{^1H\}$ NMR ($CDCl_3$, selected peaks only): δ 132 (C^4), 99 (C^1), 99 (C^2), 96 (C^6), 89 (C^5), 88 (C^{11}), 87 (C^3), 79 (C^{16}), 75 ($C^{20/17}$), 74 (C^{14}), 74 (C^{12}), 74 ($C^{17/20}$), 74 ($C^{18/19}$), 74 ($C^{19/18}$), 73 (C^{15}), 71 (C^{13}), 31 (C^8), 22 (C^{10}), 21 (C^9), 15 (C^7). $^{31}P\{^1H\}$ NMR ($CDCl_3$): δ 23.3 (d, $^2J_{PP}$ = 52, 1P, Ru-*P*Ph_3), 19.7 (d, $^2J_{PP}$ = 52, 1P, Ru-*P*Ph_2), −19.4 (s, 1P, *pend*-*P*Ph_2), −144.4 (sept,$^1J_{PF}$ = 713, 1P, *P*F_6). ESI-MS (CH_2Cl_2) positive ion: *m/z*, 533 (11%) $[M - dppf]^+$, 825 (23%) $[M - PPh_3]^+$, 1087 $[M]^+$; negative ion: *m/z*, 145 $[PF_6]^-$. Anal. Calcd for $C_{62}H_{57}ClF_6FeP_4Ru$ (1232.39 g mol^{-1}): C, 60.43; H, 4.66. Found: C, 60.38; H, 4.67.

Preparation of [RuCl(η^2-dppv)(η^6-*p*-cymene)]Cl. A solution of $[RuCl_2(\eta^6\text{-}p\text{-cymene})]_2$ (0.20 g, 0.33 mmol) and *cis*-$PPh_2CHCHPPh_2$ (0.31 g, 0.78 mmol) in CH_2Cl_2 (5 mL) was stirred at RT for 30 min. MeOH (10 mL) was added and the solution was stirred for an additional 150 min, during which time the solution became yellow. The solution was concentrated to ca. 5 mL and diethyl ether (50 mL) added. The product was then filtered, washed with diethyl ether (3 × 20 mL) and pentane (2 × 10 mL), and dried in vacuo. Yield: 0.45 g (99%). The hexafluorophosphate analogue was prepared by metathesis using $[NH_4]PF_6$ (1.2 equiv) in methanol, with a yield of 91%. NMR data are in agreement with the literature.[28] Yellow crystals of [RuCl-(η^2-dppv)(η^6-*p*-cymene)]-PF_6 suitable for X-ray diffraction were obtained by slow diffusion of diethyl ether into a CH_2Cl_2 solution of the compound at RT.

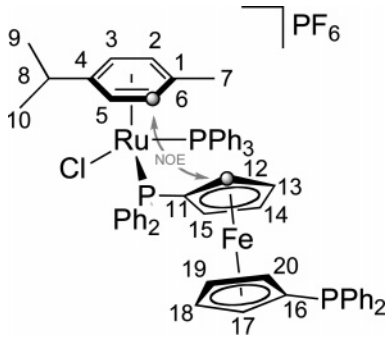

Figure 6. NMR labeling scheme for **[2e]PF$_6$** and the observed NOE interaction.

Kinetics. Chelation kinetics were monitored using ^{31}P NMR spectroscopy, integrating relative to an internal standard in sealed capillary tubes; PPh_3 in toluene for **4a** → **[5a]Cl** and **4b** → **[5b]Cl** and $PO(OEt)_3$ in toluene for **[2a−e]PF$_6$** → **[5a−e]PF$_6$**. Peaks from the resulting chelate complexes were in agreement with the literature data.[28] Integrations were preformed using NMRICMA, an iterative fitting application for MatLab.[29] Samples of **[2a−e]PF$_6$** were prepared under dinitrogen in screw cap NMR tubes. Concentrations were typically ∼20 mM. The reaction temperature was determined before and after each measurement using an external temperature probe and generally showed good agreement (±0.2 K). Additional data are listed in Tables S1 and S3.

Variable-pressure UV−visible spectrophotometric measurements for the chelation of **4a** → **[5a]Cl** and **4b** → **[5b]Cl** were performed on a Perkin-Elmer Lambda 5 spectrophotometer. A "Le Noble" piston-type cell with an optical path length of about 2 cm was used and immersed in the pressure-transmitting fluid (1:1 MeOH−CH_2ClCH_2Cl mixture) inside a pressurizable and thermostatable pressure vessel.[30] The temperature was controlled by circulation of water from a thermostat bath and measured using a Pt-resistance thermometer. Concentrations were 0.5 mM. The temperature was fixed at 298 K and the pressure varied between 1 and 1500 bar, with the rate monitored by the decrease in absorbance at 375 nm. Full data are listed in Table S2.

Kinetic measurements were made by following the reaction over, typically, three or more half-lives, and all data gave good fits to single-exponential first-order behavior (e.g., Figures S4 and S6). Errors quoted for the rate constants are the standard errors calculated from the exponential fitting. The rates of the reaction for **4a** → **[5a]Cl** and **4b** → **[5b]Cl** in 1:1 MeOH−CH_2ClCH_2Cl were within the experimental error for three different concentrations of **4b** and two of **4a**, as were duplicate measurements of each. The temperature dependence of the chelation reactions, when determined, all showed excellent Eyring behavior; see Figures S5 and S7−S11, and the quoted errors originate from the standard errors from linear fits of $\ln(k_{obs}/t)$ vs $1/T$ (i.e. $\sigma(\Delta H^{\ddagger}) = R[\sigma(\text{slope})]$, $\sigma(\Delta S^{\ddagger}) = R[\sigma(\text{intercept})]$).

(28) Jensen, S. B.; Rodger, S. J.; Spicer, M. D. *J. Organomet. Chem.* **1998**, *556*, 151−158.

(29) Helm, L.; Borel, A.; Yerly, F. *NMRICMA 3.0 for Matlab*; Institut des Sciences et Ingénierie Chimiques, EPFL Lausanne, 2004.

(30) (a) Le Noble, E. J.; Schlott, R. *Rev. Sci. Instrum.* **1976**, *47*, 770−771. (b) Richens, D. T.; Ducommun, Y.; Merbach, A. E. *J. Am. Chem. Soc.* **1987**, *109*, 603−604.

Table 6. Crystal Data and Details of the Structure Determinations

	[2a]PF_6	**[2b]PF_6**	**[2d]PF_6**	**[5b]PF_6**
formula	$C_{53}H_{51}ClF_6P_4Ru{\cdot}CH_2Cl_2$	$C_{54}H_{51}ClF_6P_4Ru$	$C_{55}H_{55}ClF_6P_4Ru{\cdot}2CH_2Cl_2$	$C_{36}H_{36}ClF_6P_3Ru{\cdot}CH_2Cl_2$
M	1147.26	1074.35	1260.24	897.00
T [K]	140(2)	100(2)	100(2)	100(2)
cryst syst	monoclinic	triclinic	monoclinic	monoclinic
space group	*P*2(1)/*n*	$P\bar{1}$	*P*2(1)/*c*	*P*2(1)
a [Å]	13.9506(7)	9.7360(19)	16.067(3)	11.162(2)
b [Å]	18.7248(11)	11.657(2)	16.140(3)	30.243(6)
c [Å]	21.1365(13)	21.649(4)	21.951(4)	11.176(2)
α [deg]		100.32(3)		
β [deg]	107.004(5)	99.40(3)	100.06(3)	91.33(3)
δ [deg]		98.34(3)		
V [Å^3]	5280.0(5)	2346.1(8)	5604.7(19)	3771.6(13)
Z	4	2	4	4
density [g cm^{-3}]	1.443	1.521	1.494	1.580
μ [mm^{-1}]	0.627	0.590	0.690	0.813
θ range [deg]	$3.05 \le \theta \le 25.03$	$3.05 \le \theta \le 25.03$	$2.91 \le \theta \le 25.03$	$3.25 \le \theta \le 25.03$
no. of measd reflns	30 281	46 107	43 673	70 101
no. of unique reflns	9226 [$R_{int} = 0.0497$]	8278 [$R_{int} = 0.0482$]	9474 [$R_{int} = 0.0451$]	13 289 [$R_{int} = 0.0442$]
no. data/restr/params	9226/38/673	8278/0/598	9474/28/747	13 289/1/907
R1, wR2 [$I > 2\sigma(I)$][a]	0.0733, 0.2201	0.0326, 0.0652	0.0624, 0.1471	0.0211, 0.0465
GoF[b]	1.061	1.110	1.119	1.119
Flack *x*				0.014(11)

[a] $R1 = \sum||F_o| - |F_c||/\sum|F_o|$, $wR2 = \{\sum[w(F_o^2 - F_c^2)^2]/\sum[w(F_o^2)^2]\}^{1/2}$. [b] $GoF = \{\sum[w(F_o^2 - F_c^2)^2]/(n - p)\}^{1/2}$ where *n* is the number of data and *p* is the number of parameters refined.

Numerical analysis was carried out using Origin 7.0 or OriginPro 7.5.[31]

Crystallography. Relevant details about the structure refinements are given in Table 6, and selected geometrical parameters are found in Table 2. Data collection for the X-ray structure determinations were performed on a KUMA CCD diffractometer system (**[2a]PF_6**) and Bruker APEX II CCD diffractometer system (**[2b]PF_6**, **[2d]PF_6**, **[5b]PF_6**) using graphite-monochromated Mo Kα radiation (0.71073 Å) and a low-tempetature device. Data reduction was performed using CrysAlis RED[32] (**[2a]PF_6**) and EvalCCD[33,34] (**[2b]PF_6**, **[2d]PF_6**, **[5b]PF_6**). Structures were solved using SIR97[35] and refined (full-matrix least-squares on F^2) using SHELXTL.[33,36] An absorption correction (SADABS) was applied to the data sets of **[2b]PF_6**, **[2d]PF_6**, and **[5b]PF_6**.[33] All non-hydrogen atoms were refined anisotropically, with hydrogen atoms placed in calculated positions using the riding model with the exception of those on C8 in **[2a]PF_6**, which were located on the Fourier difference map and then constrained. Disorder in the *p*-cymene ring of **[2a]PF_6** was satisfactorily modeled by splitting the isopropyl moiety over two sites. The $[PF_6]^-$ counterion in **[2d]PF_6** is disordered over two sites. Some of the solvent molecules in the structures of **[2a]PF_6** and **[2d]PF_6** were constrained or split over multiple sites. It was also necessary to restrain the atomic displacement parameters of some of the solvent atoms in both **[2a]PF_6** and **[2d]PF_6** and two atoms in a phenyl group of **[2d]PF_6**. Graphical representations of the structures were made with ORTEP3.[37]

Acknowledgment. We are grateful to Dr. R. Scopelliti for assistance with crystallography. We also thank the New Zealand Foundation for Research, Science and Technology for a Top Achiever Doctoral Fellowship (A.B.C.) and the EPFL and the Swiss National Science Foundation for financial support.

Note Added after ASAP Publication. In the version of this paper that appeared on the Web December 15, 2006, incorrect values appeared in Tables 4 and 5. In addition, two minor text changes were needed. The version of this paper that now appears is correct.

Supporting Information Available: Crystallographic information for **[2a]PF_6**, **[2b]PF_6**, **[2d]PF_6**, and **[5b]PF_6** in CIF format, Figures S1−S11, and Tables S1−S3. This material is available free of charge via the Internet at http://pubs.acs.org.

OM060752N

(31) *Origin 7.0* or *OriginPro 7.5*; OriginLab Corporation: Northampton, MA, 2002.
(32) *CrysAlis RED*; Oxford Diffraction Ltd.: Abingdon, Oxfordshire, U.K., 2003.
(33) Bruker AXS, Inc.: Madison, WI, 1997.
(34) Duisenberg, A. J. M.; Kroon-Batenburg, L. M. J.; Schreurs, A. M. M. *J. Appl. Crystallogr.* **2003**, *36*, 220.
(35) Altomare A.; Burla, M. C.; Camalli, M.; Cascarano, G. L.; Giacovazzo, C.; Guagliardi, A.; Moliterni, A. G. G.; Polidori, G.; Spagna, R. *J. Appl. Crystallogr.* **1999**, *32*, 115−119.
(36) Sheldrick, G. M. *SHELXTL*; University of Göttingen: Germany, 1997.
(37) Farrugia, L. J. *J. Appl. Crystallogr.* **1997**, *30*, 565.